

Weierstraß-Institut
für Angewandte Analysis und Stochastik
Leibniz-Institut im Forschungsverbund Berlin e. V.

Preprint

ISSN 2198-5855

**Thin-film electrodes for high-capacity lithium-ion batteries:
Influence of phase transformations on stress.**

Esteban Meca ¹, Andreas Münch ², Barbara Wagner ¹

submitted: April 27, 2016

¹ Weierstrass Institute
Mohrenstr. 39
10117 Berlin
Germany

E-Mail: Esteban.Meca@wias-berlin.de
Barbara.Wagner@wias-berlin.de

² Mathematical Institute
Andrew Wiles Building
University of Oxford
Oxford OX2 6GG, UK

E-Mail: muench@maths.ox.ac.uk

No. 2254
Berlin 2016



2010 *Mathematics Subject Classification.* 74N20, 35Q74, 35B25, 74S10.

Key words and phrases. Phase-Field Model, Interface Dynamics, Numerical Methods.

This research was carried out in the framework of MATHEON supported by the Einstein Foundation Berlin.

Edited by
Weierstraß-Institut für Angewandte Analysis und Stochastik (WIAS)
Leibniz-Institut im Forschungsverbund Berlin e. V.
Mohrenstraße 39
10117 Berlin
Germany

Fax: +49 30 20372-303
E-Mail: preprint@wias-berlin.de
World Wide Web: <http://www.wias-berlin.de/>

Abstract

In this study we revisit experiments by Sethuraman et al. [J. Power Sources, 195, 5062 (2010)] on the stress evolution during the lithiation/delithiation cycle of a thin film of amorphous silicon. Based on recent work that show a two-phase process of lithiation of amorphous silicon, we formulate a phase-field model coupled to elasticity in the framework of Larché-Cahn. Using an adaptive nonlinear multigrid algorithm for the finite-volume discretization of this model, our two-dimensional numerical simulations show the formation of a sharp phase boundary between the lithiated and the amorphous silicon that continues to move as a front through the thin layer. We show that our model captures the non-monotone stress loading curve and rate dependence, as observed in experiments and connects characteristic features of the curve with the structure formation within the layer. We take advantage of the thin film geometry and study the corresponding one-dimensional model to establish the dependence on the material parameters and obtain a comprehensive picture of the behaviour of the system.

1 Introduction

In recent years, interest in Lithium-ion batteries has surged. Their high energy density and their slow loss of charge make them ideal for applications ranging from portable electronics to electric cars[31, 33]. Much research is being devoted to improving its characteristics, e.g. their capacity or their charging time.

A particularly active area of research is the development of new electrodes. Typically, Li-ion batteries consist of an anode of graphite and a cathode of a lithium compound, but other materials are being proposed. In particular, silicon is heralded as a very promising alternative to graphite. When charging, lithium is stored in the anode, and silicon electrodes can store as much as ten times more lithium than their graphite counterparts[22].

Nevertheless, the use of silicon as an electrode material presents a number of challenges[22]. To begin with, its volume increases by about 300% when fully lithiated[1, 25], and hence the material is subject to enormous stresses that cause the mechanical failure and the destruction of the electrode after a small number of charge-discharge cycles. To overcome this difficulty, structures such as nanopillars[15] or nanowires[6] are being investigated, with promising results[10].

In order to optimize the geometry and nanopatterning of the electrodes, it is essential to understand the material properties of silicon under heavy lithiation and this has been the subject of extensive experimental and theoretical research in recent years. It seems to be well established that after the first lithiation-delithiation cycle, crystalline silicon becomes amorphous[22], and hence the relevant material to study is amorphous silicon. In that respect, it has been proven that the first lithiation of crystalline as well as amorphous silicon occurs initially through a two-phase mechanism[21, 32], but it is still controversial whether this two-phase mechanism is also present for amorphous silicon in subsequent lithiations[19, 21]. A recent first-principles study[7] relates the two-phase lithiation of amorphous silicon with a structural transition that would occur

for a lithium molar fraction $x \approx 2$. Experiments show that this two-phase lithiation is self-limiting in nanowires [19], presumably due to the high stresses generated.

Moreover, it has been found that amorphous silicon behaves plastically when lithiated[2, 26, 27], which seems surprising for a material which also fractures in a brittle manner.

These unusual characteristics have sparked a minor controversy. The maximum stress measured in the experiments does not reach the predicted yield stress for amorphous silicon[28], and this seems to forbid any plastic behaviour, against the experimental evidence. There have been some attempts at explaining this. On the one hand, there is the idea of reactive flow[35], by which lithiated silicon could flow plastically below the yield point. In accordance with this idea, a phenomenological yield stress function that incorporates the effects of lithium concentration has been proposed[35]. While this theory is able to reproduce approximately the hysteresis loop for stress, it still has problems to accommodate the linear relationship observed between the observed stress and the charging rate[26].

An alternative theory[17, 18] involves the dependency of the chemical potential on deviatoric stresses. Using a generalized chemical potential, which changes discontinuously with the sign of the rate of change of the lithium molar fraction, good agreement with the experimental curve has been demonstrated, even though this comparison is obtained through a fit.

Additional problems arise when considering the modelling of plasticity. As of now, only simple viscoplastic flow laws have been considered. These are based on power laws of stress and give exponents ranging from 5 to 50 [2, 3], suggesting that a piece may be missing from the model.

In this article we revisit the experiments determining the plastic behaviour [26, 27] and study the effect of the formation of a highly lithiated phase in amorphous silicon. Results in Refs. [7, 32] suggest that strong gradients and even phase separation may be present in the experiments. We thus discuss qualitatively the value of the average stress that would be found as a function of concentration using our phase-field model that exhibit characteristic properties of the loading curve that have been previously identified with yielding. Our approach also brings charging-rate dependence into the problem, as well as hysteresis, as this is implicit in any phase-separation phenomenon. This suggests that the inhomogeneity of the electrode might be the underlying cause for many of the observed features.

We model the thin electrode of Ref. [27] as a thin layer attached to a fixed substrate. Our modelling approach starts from the Cahn-Hilliard-Reaction equation[29] commonly used for lithium intercalation dynamics, and includes linear elasticity, following the Larché-Cahn[14] prescription. We note that while we have made this choice for simplicity, as it is one of the simplest models that couples consistently phase separation dynamics with elasticity, it will allow only for qualitative comparison with experimental results.

In Section 2 we introduce the model and the assumptions behind it, as well as the relevant non-dimensional parameters. In Section 3 we give a detailed study of the dependency of the stress loading curve on the different parameters, and in Section 4 we discuss the results and present our conclusions.

2 The Model

We are interested in the dynamics of the system described in Ref. [27]; a schematic is shown in Fig. 1. Lithium is absorbed from an electrolyte by a thin layer of amorphous silicon (a-Si) sitting

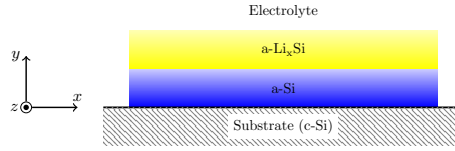


Figure 1: Schematic of the system.

on a non-deformable substrate. When the lithium concentration is high enough, the layer separates into a Li-rich phase (a-Li_xSi) and the a-Si phase with no or very low lithium concentration. For the purpose of formulating the model equations, we assume that the layer is bounded in the x direction, and we work within the plane strain approximation. The equations can therefore be formulated effectively in a two-dimensional rectangular domain Ω , although later we will also consider the one-dimensional case. Coordinates $x \equiv x_1$, $y \equiv x_2$, and $z \equiv x_3$ are introduced as indicated in the schematic, and t represents time. The indices of the tensors run from 1 to 3 and summation is implied over repeated indices.

We assume that lithium ions are slowly absorbed in an electrode held at constant temperature. Lithium ions become neutral on a thin boundary layer, when entering the electrode from the electrolyte. The insertion of lithium causes an isotropic stress-free strain ϵ_{ij}^0 that will depend on the concentration of lithium atoms c . We assume that the stress-free strain can be written as $\epsilon_{ij}^0 = \alpha h(c/c_{\max}) \delta_{ij}$, where the constant α is the maximum stress-free strain and c_{\max} is the lithium concentration in the a-Li_xSi phase, and h interpolates between $h(0) = 0$ and $h(1) = 1$. We will typically use a linear function for h .

The medium is considered to be amorphous, and hence assumed to be isotropic. We use linear elasticity for simplicity, so that the elastic energy density has the form:

$$W = \frac{1}{2} C_{ijkl} (\epsilon_{ij} - \epsilon_{ij}^0) (\epsilon_{kl} - \epsilon_{kl}^0), \quad (1)$$

(summation implied) where C_{ijkl} is the fourth-order elasticity tensor and ϵ_{ij} is the strain tensor, defined in terms of the deformation \mathbf{u} as follows:

$$\epsilon_{ij} = \frac{1}{2} (\partial_j u_i + \partial_i u_j). \quad (2)$$

The previous elastic energy implies the following definition of stress:

$$\sigma_{ij} = C_{ijkl} (\epsilon_{kl} - \epsilon_{kl}^0), \quad (3)$$

where the symmetries of the elasticity tensor have been used. Finally, we consider the plane strain approximation, and hence $\epsilon_{i3} = 0$.

In order to model the coupled system, we include the elastic energy (1) in a free energy functional of the following form:

$$\mathcal{F} = N_\Omega \int_\Omega \left(\frac{1}{2} \gamma \epsilon |\nabla c|^2 + \frac{\gamma}{\epsilon} f(c) + W(\epsilon_{ij}, c) \right) dx dy, \quad (4)$$

where the homogeneous free energy density f has a double well form (a specific choice will be made later) and $W(\epsilon_{ij}, c)$ is the elastic energy density as defined in Eq. (1). The constant γ carries the dimensions of energy times length, N_Ω is the (global) number of particles in Ω and the parameter ϵ is related to the interface thickness.

We introduce the chemical potential,

$$\mu = \frac{1}{N_{\Omega}} \frac{\delta \mathcal{F}}{\delta c} = -\gamma \epsilon \nabla^2 c + \frac{\gamma}{\epsilon} f'(c) + \partial_c W(\epsilon_{ij}, c), \quad (5)$$

and postulate the following evolution equation for the concentration:

$$\partial_t c = \nabla \cdot (M(c) \nabla (\mu + \chi \epsilon \partial_t c)). \quad (6)$$

The mobility function $M(c)$ can in general be a function of the concentration, but here we will only consider the case where it is a constant, $M(c) \equiv M$. The last term is the viscous term, [see 24] and χ corresponds to a parameter with dimensions of viscosity. This term is associated with the inclusion of non-local equilibrium interfacial kinetics [9, 12]. The scaling with ϵ of each term has been chosen to make sure that we obtain the correct asymptotic sharp-interface limit, see Ref. [23] for details.

Eqns. (5), (7), together with the mechanical equilibrium condition

$$\partial_j \sigma_{ij} = 0, \quad (7)$$

constitute the core of our model. They are supplemented with boundary conditions, which are no deformation and no flux at the substrate and traction free and fixed flux (F) boundary conditions at the electrolyte. They will be formulated explicitly in non-dimensional form at the end of this section.

Nondimensionalization

We adapt the nondimensionalization from Ref. [16]. For characteristic length scale L_0 we choose the thickness of the amorphous silicon layer, concentrations are scaled by their maximum value c_{math} , $G_0 = E_{\text{Si}}/[2(1 + \nu)]$ is the shear modulus of pure amorphous silicon and is used to scale the shear modulus which is also assumed to depend on the concentration. The constants and E_{Si} and ν are Young's modulus for pure amorphous silicon and Poisson's ratio. The scalings are

$$\begin{aligned} \mu &\rightarrow \tilde{\mu} \gamma L_0^{-1}, & x &\rightarrow \tilde{x} L_0, & t &\rightarrow \tilde{t} L_0^3 M^{-1} \gamma^{-1}, \\ \epsilon &\rightarrow \tilde{\epsilon} L_0, & u_i &\rightarrow \tilde{u}_i L_0 \alpha, & C_{ijkl} &\rightarrow \tilde{C}_{ijkl} G_0, \\ \sigma_{ij} &\rightarrow \tilde{\sigma}_{ij} G_0, & \epsilon_{ij} &\rightarrow \tilde{\epsilon}_{ij} \alpha, & c &\rightarrow \tilde{c} c_{\text{max}}. \end{aligned} \quad (8)$$

With these scalings, we obtain

$$\partial_t c = \nabla^2 (\mu + \epsilon X \partial_t c), \quad (9a)$$

$$\mu = -\epsilon \nabla^2 c + \frac{1}{\epsilon} f'(c) + Z \partial_c W(\epsilon_{ij}, c), \quad (9b)$$

$$\partial_j \sigma_{ij} = 0. \quad (9c)$$

in the bulk. The constitutive law for the stress takes the form,

$$\sigma_{ij} = 2G(c) (\epsilon_{ij} - \epsilon_{ij}^0) + \frac{2\nu}{1 - 2\nu} G(c) (\epsilon_{kk} - \epsilon_{kk}^0) \delta_{ij}, \quad (9d)$$

where

Table 1:

$$\epsilon_{ij}^0 = h(c)\delta_{ij}, \quad (9e)$$

$$G(c) = 1 + g(c) \left(\frac{E_{\text{Li}_x\text{Si}}}{E_{\text{Si}}} - 1 \right). \quad (9f)$$

The constant $E_{\text{Li}_x\text{Si}}$ is Young's modulus for fully lithiated amorphous silicon and $g(c)$ interpolates between $g(0) = 0$ and $g(1) = 1$. In this paper, we specifically choose g to be linear. We also have

$$\mathbf{u} = 0, \quad \mathbf{n} \cdot \nabla c = 0, \quad \mathbf{n} \cdot \nabla \mu = 0, \quad (9g)$$

at the electrode-substrate boundary, and so-called variational boundary conditions[4] at the top electrode-electrolyte boundary

$$\sigma \cdot \mathbf{n} = 0, \quad \mathbf{n} \cdot \nabla c = 0, \quad \mathbf{n} \cdot \nabla \mu = Y, \quad (9h)$$

with a constant, non-dimensional flux Y . In the present form we neglect the dependency of the surface reptionenergy on concentration. At the two lateral boundaries of the layer, we impose the same conditions except that we set the flux to zero.

We have six dimensionless parameters, namely

$$X = \frac{\chi M}{L_0}, \quad Y = \frac{FL_0^2}{M\gamma}, \quad Z = \frac{L_0 E_{\text{Si}} \alpha^2}{2(1 + \nu)\gamma},$$

the ratio of the Young moduli $E_{\text{Li}_x\text{Si}}/E_{\text{Si}}$, Poisson's ratio ν , and the scaled interface thickness ϵ .

3 Results

We numerically study the model described by Eqs. (9) in one and two dimensions via an adaptive nonlinear multigrid algorithm and the solver BSAM[34]. We use a Crank-Nicolson scheme for the time stepping, and discretize the equations with a finite-volume scheme to enforce the conservation of Li.

Approximate values for some of the parameters can be obtained from the literature. From Ref. [28], we obtain $E_{\text{Li}_x\text{Si}}/E_{\text{Si}} = 4/9$ for the ratio of the Young moduli and $\nu = 0.25$ for Poisson's ratio. We assume that we can neglect the dependency of ν on the lithium concentration. The interface thickness is taken to be 1.25nm, which is in line with the sharp interface observed in experiments[32]. For a layer thickness $L_0 = 250\text{nm}$, we obtain $\epsilon = 0.005$. By assuming that the high concentration of Li during phase separation corresponds to a-Li_{2.5}Si, as it has been reported[32], we obtain a value of $\alpha = 0.62$ following Ref. [2]. The remaining parameters are characteristic of this transition that remains mostly unknown, and hence we cannot fix the values of X , Y and Z . For this reason, we study the effect of varying these parameters, see Section 3 below.

Finally, we choose $h(c) = g(c) = c$ and $f(c) = c^2(1 - c)^2/4$ for simplicity. Below we show that the results will necessarily depend quantitatively on the form of f , but we expect to capture

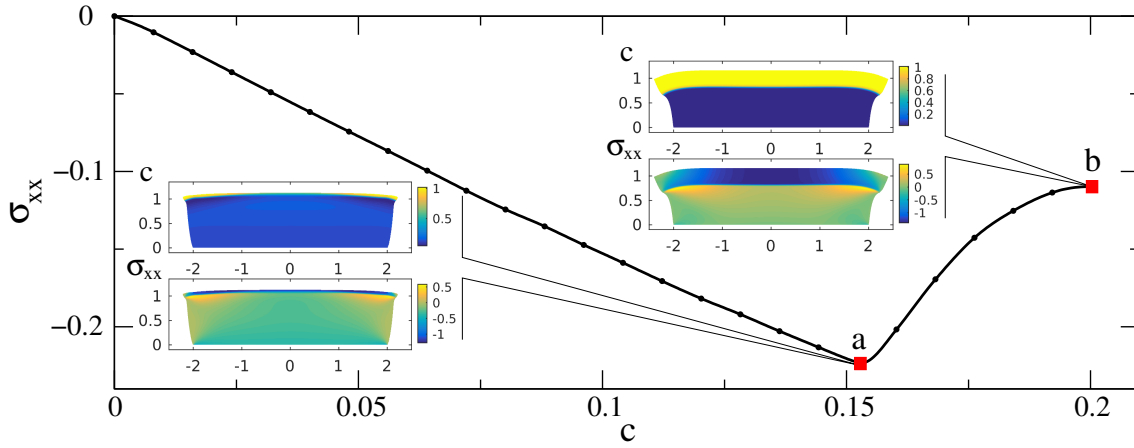


Figure 2: Initial loading process for $Z = 0.1$, $X = 0.5$, $Y = 0.01$ (color online). Loading curve, with points (a) and (b) marked (see text). Insets: concentration field and σ_{xx} field at points (a) and (b). The non-dimensional deformation has been exaggerated to help its visualization.

the qualitative behaviour. We discuss below the bounds of the non-dimensional numbers based on this form of f .

To illustrate the behaviour of the system, we solved the equations for a layer with a moderate aspect ratio. The results are displayed in Fig. 2.

The stress loading curve (referred to as *loading curve* from now on) shows the average σ_{xx} vs. the average concentration on Ω as the electrode is loaded. At the beginning, the stress grows linearly with the concentration (i.e. it becomes more negative, compressive), but at a certain concentration, marked as point (a) the regime changes abruptly, until it reaches a maximum, marked as point (b).

To understand this behaviour we display on the right hand side of Fig. 2 the concentration field and the σ_{xx} field at the points (a) and (b). As we see, at point (a) phase separation is beginning, starting from the sides (a two-dimensional effect), and negative stress is localized in the highly lithiated phase. As the concentration is increased from point (a) to point (b), phase separation is completed and we are left with two definite layers with an abrupt change of concentration between them.

Notice that the loading curve has a marked minimum, but unlike in the experiments of Ref. [27], this minimum does not correspond to the yield point of the material, but rather to simple *stress localization*: As the system phase-separates, lithium and hence stress are concentrated in a thin layer with a smaller value of Young's modulus than a-Si. Hence, average stress becomes less compressive, but in fact the stresses are much higher in this thin layer than they were before the onset of phase separation.

This behaviour can be understood further by considering Fig. 3. In this figure we display the average concentration and σ_{xx} on a cross section at $x = 0$. It shows that at an early stage, when the average concentration is somewhat smaller than at (a), we have an almost flat curve, with a slightly higher concentration at the interface with the electrolyte (at $y = 1$), and the stress is almost constant. At point (a), the concentration increases much more rapidly near $y = 1$ than in other parts of the layer, thus signalling the start of a phase-separation process. The stress becomes very negative near $y = 1$, as the concentration is also localized there. Finally, phase-separation is completed at point (b), and we can observe a very well-defined layer with high

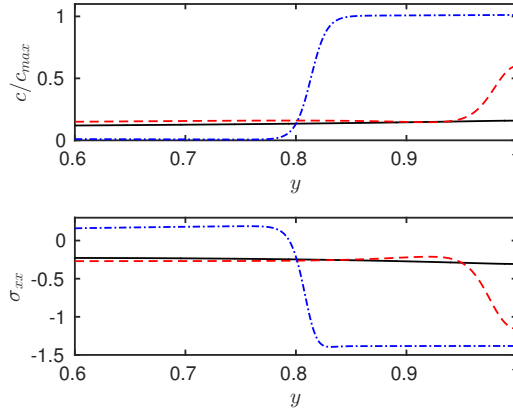


Figure 3: Concentration and stress in the cross section at $x = 0$, for different values of the average concentration, same parameters as Fig. 2 (color online). In black (solid), a line for $c/c_{max} = 0.120$, before point (a). The red (dashed) line corresponds to the point (a) in Fig. 2, and the blue (dash-dotted) to the point (b).

concentration and very large negative stress.

So far we have presented the results for a single set of parameters. In the following section we turn to the one-dimensional case to investigate more easily if these features are generic or depend strongly on the parameters.

Parameter study for the one-dimensional system

The layer of a-Si that acts as an electrode has a thickness of 250nm and the wafer has a diameter of 3 inches (and the curvature is small enough, so we can consider it locally flat). Hence, the problem is one-dimensional to very good approximation. In fact, this is true even for the results in Fig. 3 despite the moderate aspect ratio used there. Also, the one-dimensional formulation is more fundamental. It is independent of the specific model for the interaction with the electrolyte, as the flux is imposed externally and has no lateral variations..

The model equations (9) can be reduced to their one-dimensional form by dropping all dependencies on x and assuming that the lateral displacement $u_x = 0$. This immediately leads to $\sigma_{xy} = 0$. By using Eq. (9c) and boundary conditions (9h) we obtain $\sigma_{yy} = 0$, and

$$\epsilon_{yy} = \frac{1 + \nu}{1 - \nu} h(c), \quad (10)$$

$$\sigma_{xx} = -2G(c) \frac{1 + \nu}{1 - \nu} h(c), \quad (11)$$

i.e. we can express all the elastic properties in terms of the concentration. Furthermore, using $h(c) = g(c) = c$ we can express the chemical potential as

$$\mu = -\epsilon \partial_y^2 c + \frac{1}{\epsilon} f'(c) - 2Z \frac{1 + \nu}{1 - \nu} \left[3c^2 \left(1 - \frac{E_{\text{Li}_x\text{Si}}}{E_{\text{Si}}} \right) - 2c \right]. \quad (12)$$

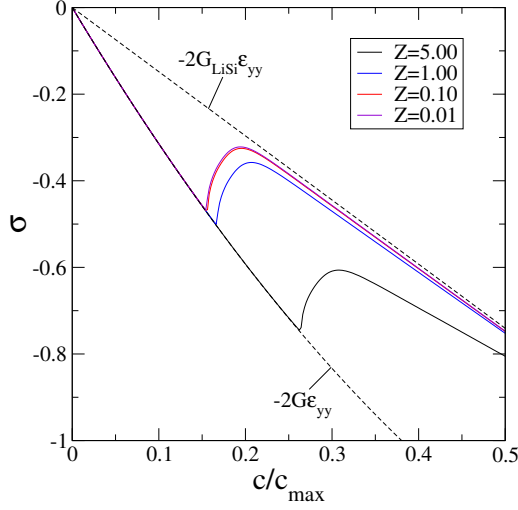


Figure 4: Effect of varying Z (color online), for $X = 0.5$, $Y = 0.02$. The solid lines represent loading curves for different values of Z . The lower dashed line corresponds to a single phase uniform system being lithiated. The upper dashed line corresponds to a two-phase lithiation process where all of the stress is localized in the lithiated phase.

This equation shows that the dynamics of the concentration (e.g. the point at which the system will phase separate) depends on the interaction of the last term with the double-well free energy, as stated above.

The qualitative study of (12) shows that the effect of the coupling is to leave the energy of pure a-Si unchanged, and raise the energy associated with the fully lithiated state. Hence we can anticipate that the higher the value of Z , the higher the value of c at which phase separation occurs will be. It is easy to compute the stability of a uniform profile of concentration in the limiting case of low flux (see Appendix A). The main result of this stability analysis confirms indeed that the coupling with elasticity delays phase separation, and there is a linear relation between the concentration at the onset and Z for $\epsilon \ll 1$ (see Eq. 17).

Fig. 4 displays several loading curves for different values of Z . For small values of the concentration, the curve follows very closely the curve that would be expected for a uniform layer, Eq. (11). Nevertheless, at a certain point the system begins to phase-separate and goes into a different regime. In this regime, phase separation is complete (cf. point (b) in Fig. 2). Then, since most of the stress is located in the lithiated layer and it is approximately constant, the average stress will be this value of stress times the ratio of the thickness of the lithiated layer over the total thickness, i.e. the average concentration. The stress on the lithiated layer can be found from Eq. (11) for $c = 1$, and the average stress is this value times the average concentration. This relation is depicted in Fig. 4 as the upper dashed line.

For μ to remain physically meaningful, the value of Z cannot be too high, to ensure that the term coming from the elastic energy remains small compared with f . Again, the particular value of Z at which the results will not be meaningful will depend on the particular form of f . We see in Fig. 4 that phase separation occurs at higher values of the concentration with increasing Z , as expected from Eq. (17). We note that the curve for $Z = 5$ clearly behaves differently, meaning that for this value the perturbation caused by elasticity to μ cannot be considered small anymore. We also remark that the values of the remaining parameters in Fig. 4 are not important to illustrate this dependence as it is observed for all values.

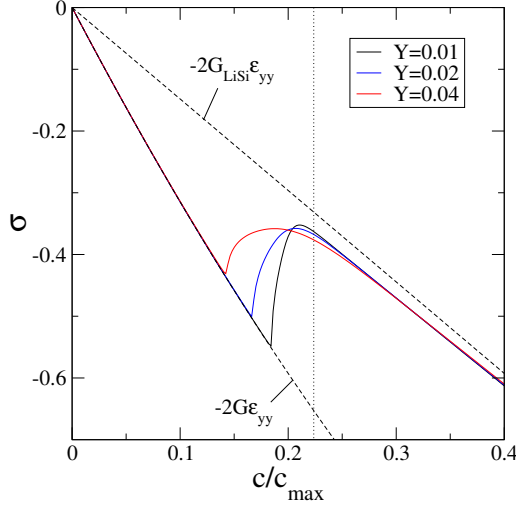


Figure 5: Effect of varying the nondimensional flux Y (color online) for $X = 0.5$, $Z = 1.0$. Solid lines correspond to different values of Y , dashed lines are limiting cases, as in Fig. 4. The dotted vertical line corresponds to the concentration at the spinodal line, $c = 0.2237$.

Fig. 5 shows the variation of the loading curve with non-dimensional flux Y . Phase separation occurs more abruptly and at a higher concentration as Y is decreased. For reference we show in Fig. 5 the concentration at which a uniform concentration would be unstable and undergo spinodal decomposition for $Z = 1.0$ (see Appendix A). Clearly, the smaller the flux is the more uniform the concentration in the electrode will be, and therefore the closer the critical concentration will be to the critical concentration for the uniform system. This is a form of rate dependence of the loading curve, i.e. dependence on the rate of charge.

The parameter Y is the only one that in principle is controllable in experiments. For a small enough value of the flux, we will observe the behaviour described in Fig. 5, as there is an absolute limit of the concentration at which the uniform system is unstable, hence the behaviour described is robust for at least an interval of values of Y . Also, if the flux is too high, the system jumps immediately into the phase separated regime, which corresponds to a straight line. Again, the qualitative outcome does not change if we vary the other parameters. Higher Z shifts the value of the transition point towards higher concentrations, but the tendency will be the same.

To study the effect of the kinetic parameter X we also varied its value four orders of magnitude, see Fig. 6. The overall effect of increasing X is to delay phase separation. When its value is high enough, the extrema of the loading curve disappear (see the line for $X = 10$).

The delay of phase separation for increasing kinetic parameter values is to be expected. On the one hand, the growth rate of the instability of the uniform case is reduced for larger values of X (see Appendix A). On the other hand, the delay in the instability can be expected on more general grounds. In order to grow in the presence of interface friction, which in this model comes from the inclusion of the viscous term, a driving force is needed to counteract this process. This is provided by the inequality of the chemical potentials of the diffusing species, and this implies that the concentration of the growing phase has to be higher than it would be in local equilibrium conditions[13]. This implies that a higher average concentration is needed for phase separation, which will therefore be delayed.

The correct value of the kinetic parameter is unknown, as it is not directly accessible experimentally. Nevertheless, like Z , its value should not be too high for the present model to be valid.

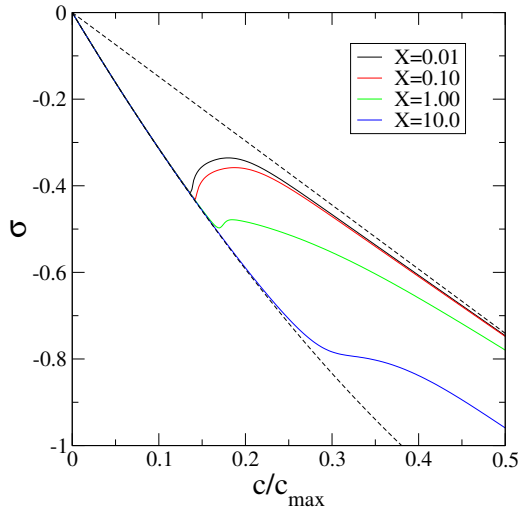


Figure 6: Effect of varying the nondimensional kinetic parameter X (color online) for $Y = 0.04$, $Z = 1.0$. Solid lines correspond to loading curves with different values of X . Dashed lines correspond to limiting cases (see Fig. 4).

We see in Fig. 6 already that for $X = 10$ we obtain an extreme change of behaviour, which indicates again that for this value the viscous term is far from being a small perturbation.

4 Discussion

We have found that taking into account the possibility of phase-separation dynamics for a lithiated electrode introduces new phenomena that could help explain some of the puzzling features found in experiments. Some of the consequences of two-phase lithiation of a-Si have indeed been found in experiments[21, 32].

Our model is a valuable tool to study the effect of phase separation in our system qualitatively. We see that it can lead to a non-monotone behaviour of the loading curve without requiring plasticity, to a dependency on the rate of lithiation and to a hysteresis cycle.

For illustration purposes, we depict in Fig. 7 a hysteresis loop, which is present, as expected, in the phase separating system. The electrode is charged with a positive value of the flux ($Y = 0.02$) until it phase-separates. Then the flux is reversed, and the stress curve goes parallel to the upper dashed line, which corresponds to a fully phase-separated electrode. Before reaching concentration zero the system becomes nearly homogeneous again, thus closing the loop.

Our one-dimensional parameter study shows that phase separation is almost always present, except perhaps for very high values of Z or X (see Figs. 4 and 6). These high values would require in any case a more accurate model for f and the kinetics in any case.

In addition, the large volume changes, estimated to be about 280%[25], are beyond the limit of applicability of linear elasticity and finite strain effects need to be taken into account. Nevertheless, our results on stress localization, even if not quantitative, should still be valid.

Moreover, it is important to point out that we cannot discard plasticity as an important effect in this system. On the contrary, stress localization would indeed produce very large compressive stresses that could reach the yield point of the material. The challenge is to explain the fact that

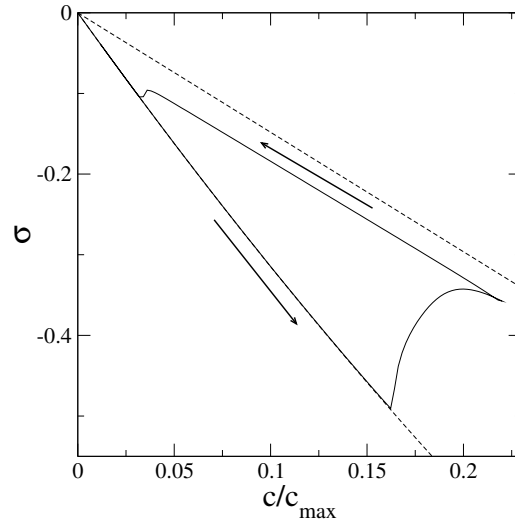


Figure 7: Hysteresis loop for $X = 0.05$, $Y = \pm 0.02$, $Z = 1.0$. When the maximum charge desired is reached, the flux is reversed. See Fig. 4 for the upper and lower dashed lines.

the value of the yield stress from Ref. [27] is significantly lower than the one expected[17], and large gradients and two-phase lithiation may have to be taken into account to understand this problem.

The phase-field model in this paper does not attempt to be quantitatively correct and capture all the physical effects. The quantitative results depend, for example, on the precise form of the free energy f . We have, however, taken care so that we remain consistent with the correct sharp interface limit[23], and have focused on results and trends that are robust and do not depend on the form of f or similar details. In particular, if phase separation is indeed present in the lithiation/delithiation process, stress localization would be a necessary consequence, independent of the detailed phase separation model. Regarding phase separation, while experiments do not show it explicitly, they show indeed two-phase lithiation[21, 32] and theoretical calculations show an abrupt change in material properties as lithium concentration is increased[7]. Hence, even in the absence of phase separation dynamics, two-phase lithiation and the corresponding stress localization should be taken into account in the interpretation of the experiment of Ref. [27].

Finally, we consider phase separation between amorphous phases, such as the ones found in amorphous silicon for high pressure[8] or in bulk metallic glasses[20]. The results for our model (9) predict that the coupling with elasticity hinders phase separation (see Appendix A). This observation is a natural result of how a coherency strain (i.e. a strain due to the deformation of the lattice) is developed in a solid solution for a crystalline material[5]. Nevertheless, it is not clear that this effect of the strain on the phase separation is necessarily present in amorphous systems[30], where the picture is more complicated. This topic will be left to future research.

In summary, we make the case that phase-separation dynamics and two-phase lithiation could play an important role in the interpretation of the discussed experiments. In order to have a more realistic representation of the experiments, we are presently implementing a model that incorporates nonlinear elasticity, plasticity and a more detailed electrochemical modeling.

A Linear Stability of the One-Dimensional Model

In order to help the discussion, we develop in this appendix a linear stability analysis of the one-dimensional problem, which is defined by Eq. (9a) with the chemical potential given by Eq. (12). Here we reproduce the classic result by Cahn[5] for spinodal decomposition of a solid solution, slightly augmented with the effect of kinetics. For a review on spinodal decomposition and first-order phase transitions see Ref. [11].

We consider a constant solution of Eq. (12), $c = c_0$. This solution is in principle attainable in the limit of zero flux. With this solution, Eq. (12) can be easily linearized about it:

$$\partial_t c = \nabla^2 \left\{ \frac{1}{\epsilon} f''(c_0) c - \epsilon \nabla^2 c + \epsilon X \partial_t c - 2Z \frac{1+\nu}{1-\nu} \left[6c_0 \left(1 - \frac{E_{\text{Li}_x\text{Si}}}{E_{\text{Si}}} \right) - 2 \right] c \right\}, \quad (13)$$

where we have removed the terms that are immediately zero.

For an ansatz of the form

$$c(y, t) = e^{\lambda t} \cos(ky), \quad (14)$$

we obtain the following dispersion relation:

$$\lambda = \frac{-k^2}{1 + \epsilon X k^2} \left\{ \frac{1}{\epsilon} f''(c_0) + \epsilon k^2 - 2Z \frac{1+\nu}{1-\nu} \left[6c_0 \left(1 - \frac{E_{\text{Li}_x\text{Si}}}{E_{\text{Si}}} \right) - 2 \right] \right\}. \quad (15)$$

We see already that X will decrease the growth rate. The critical concentration does not depend on X but will depend on the particular form of the potential. Clearly, for $Z = 0$ we obtain the standard result that the instability occurs for $f''(c_0) < 0$, beginning with high wavenumbers. Setting $\lambda = 0$ in Eq. (15), using $f(c) = c^2(1-c)^2/4$, and taking $k = \pi$ (lowest lying mode for the Neumann problem in $[0, 1]$) we obtain the following value for the critical concentration:

$$c_{0,c} = \frac{1}{2} - 2\epsilon abZ \pm \frac{1}{6} \sqrt{3 + 24\epsilon bZ (6a^2 bZ \epsilon - 3a - 2) - 12\pi^2 \epsilon^2}, \quad (16)$$

where $a = (E_{\text{Li}_x\text{Si}}/E_{\text{Si}} - 1)$ and $b = (1 + \nu)/(1 - \nu)$. The previous equation gives two points on the so-called *strain* or *coherent spinodal*[5] for this problem. We can prove easily for small values of ϵ that the coupling with elasticity hinders phase separation, as expected. If we take the smallest value in Eq. (16) (corresponding to the minus sign) and expand it in powers of ϵ we obtain:

$$c_{0,c} = \frac{1}{6} (3 - \sqrt{3}) + \frac{2}{3} [3(\sqrt{3} - 1)a + 2\sqrt{3}] bZ\epsilon + O(\epsilon^2). \quad (17)$$

The first term of this equation corresponds to the lower concentration at which $f''(c) = 0$. We can write down the first order term as a function of the original parameters:

$$\left[2(\sqrt{3} - 1) \frac{E_{\text{Li}_x\text{Si}}}{E_{\text{Si}}} - \frac{2\sqrt{3}}{3} + 2 \right] \frac{1 + \nu}{1 - \nu} \epsilon Z, \quad (18)$$

and it is indeed greater than zero, as expected. This means that spinodal decomposition will develop at higher values of the concentration.

References

- [1] LY Beaulieu, KW Eberman, RL Turner, LJ Krause, and JR Dahn. Colossal reversible volume changes in lithium alloys. *Electrochemical and Solid-State Letters*, 4(9):A137–A140, 2001.
- [2] Allan F Bower, Pradeep R Guduru, and Vijay A Sethuraman. A finite strain model of stress, diffusion, plastic flow, and electrochemical reactions in a lithium-ion half-cell. *Journal of the Mechanics and Physics of Solids*, 59(4):804–828, 2011.
- [3] Giovanna Bucci, Siva PV Nadimpalli, Vijay A Sethuraman, Allan F Bower, and Pradeep R Guduru. Measurement and modeling of the mechanical and electrochemical response of amorphous Si thin film electrodes during cyclic lithiation. *Journal of the Mechanics and Physics of Solids*, 62:276–294, 2014.
- [4] Damian Burch and Martin Z. Bazant. Size-dependent spinodal and miscibility gaps for intercalation in nanoparticles. *Nano Letters*, 9(11):3795–3800, 2009. PMID: 19824617.
- [5] John W Cahn. On spinodal decomposition. *Acta metallurgica*, 9(9):795–801, 1961.
- [6] Candace K Chan, Hailin Peng, Gao Liu, Kevin McIlwrath, Xiao Feng Zhang, Robert A Huggins, and Yi Cui. High-performance lithium battery anodes using silicon nanowires. *Nature nanotechnology*, 3(1):31–35, 2008.
- [7] Ekin D. Cubuk and Efthimios Kaxiras. Theory of structural transformation in lithiated amorphous silicon. *Nano Lett.*, 14(7):4065–4070, Jul 2014.
- [8] Dominik Daisenberger, Mark Wilson, Paul F McMillan, Raul Quesada Cabrera, Martin C Wilding, and Denis Machon. High-pressure x-ray scattering and computer simulation studies of density-induced polyamorphism in silicon. *Physical Review B*, 75(22):224118, 2007.

- [9] Wolfgang Dreyer and Clemens Gohlke. Sharp limit of the viscous cahn–hilliard equation and thermodynamic consistency. *Continuum Mechanics and Thermodynamics*, pages 1–22, 2015.
- [10] H Föll, H Hartz, E Ossei-Wusu, J Carstensen, and O Riemenschneider. Si nanowire arrays as anodes in li ion batteries. *physica status solidi (RRL)-Rapid Research Letters*, 4(1-2):4–6, 2010.
- [11] J.D Gunton, M. San Miguel, and P.S. Sahni. The dynamics of first order phase transitions. In *Phase Transitions and Critical Phenomena*, volume 8, pages 269–466. Academic Press, 1983.
- [12] Morton E Gurtin. Generalized ginzburg-landau and cahn-hilliard equations based on a microforce balance. *Physica D: Nonlinear Phenomena*, 92(3):178–192, 1996.
- [13] M Hillert and M Rettenmayr. Deviation from local equilibrium at migrating phase interfaces. *Acta materialia*, 51(10):2803–2809, 2003.
- [14] F Larché and John W Cahn. A linear theory of thermochemical equilibrium of solids under stress. *Acta Metallurgica*, 21(8):1051–1063, 1973.
- [15] Seok Woo Lee, Matthew T. McDowell, Jang Wook Choi, and Yi Cui. Anomalous shape changes of silicon nanopillars by electrochemical lithiation. *Nano Letters*, 11(7):3034–3039, July 2011.
- [16] PH Leo, JS Lowengrub, and Heng-Jeng Jou. A diffuse interface model for microstructural evolution in elastically stressed solids. *Acta materialia*, 46(6):2113–2130, 1998.
- [17] Valery I. Levitas and Hamed Attariani. Anisotropic compositional expansion and chemical potential for amorphous lithiated silicon under stress tensor. *Sci. Rep.*, 3, Apr 2013.
- [18] Valery I. Levitas and Hamed Attariani. Anisotropic compositional expansion in elastoplastic materials and corresponding chemical potential: Large-strain formulation and application to amorphous lithiated silicon. *Journal of the Mechanics and Physics of Solids*, 69:84–111, Sep 2014.
- [19] Xiao Hua Liu, Feifei Fan, Hui Yang, Sulin Zhang, Jian Yu Huang, and Ting Zhu. Self-limiting lithiation in silicon nanowires. *ACS Nano*, 7(2):1495–1503, Feb 2013.
- [20] Norbert Mattern, Ulla Vainio, Jin Man Park, Jun Hee Han, Ahmed Shariq, Do Hyang Kim, and Jürgen Eckert. Phase separation in $\text{Cu}_{46}\text{Zr}_{47-x}\text{Al}_7\text{Gd}_x$ metallic glasses. *Journal of Alloys and Compounds*, 509:S23–S26, 2011.
- [21] Matthew T McDowell, Seok Woo Lee, Justin T Harris, Brian A Korgel, Chongmin Wang, William D Nix, and Yi Cui. In situ tem of two-phase lithiation of amorphous silicon nanospheres. *Nano letters*, 13(2):758–764, 2013.
- [22] Matthew T McDowell, Seok Woo Lee, William D Nix, and Yi Cui. 25th anniversary article: Understanding the lithiation of silicon and other alloying anodes for lithium-ion batteries. *Advanced Materials*, 25(36):4966–4985, 2013.

- [23] Esteban Meca, Andreas Münch, and Barbara Wagner. Sharp-interface formation during lithium intercalation into silicon. Preprint XXX, Institute of Mathematics, Technical University Berlin, 2016.
- [24] A Novick-Cohen. On the viscous Cahn-Hilliard equation. Material instabilities in continuum mechanics, Edinburgh, 1985–1986, 329–342. *Oxford Sci. Publ., Oxford Univ. Press, New York*, 1988.
- [25] MN Obrovac and LJ Krause. Reversible cycling of crystalline silicon powder. *Journal of The Electrochemical Society*, 154(2):A103–A108, 2007.
- [26] Matt Pharr, Zhigang Suo, and Joost J Vlassak. Variation of stress with charging rate due to strain-rate sensitivity of silicon electrodes of li-ion batteries. *Journal of Power Sources*, 270:569–575, 2014.
- [27] Vijay A Sethuraman, Michael J Chon, Maxwell Shimshak, Venkat Srinivasan, and Pradeep R Guduru. In situ measurements of stress evolution in silicon thin films during electrochemical lithiation and delithiation. *Journal of Power Sources*, 195(15):5062–5066, 2010.
- [28] VB Shenoy, P Johari, and Y Qi. Elastic softening of amorphous and crystalline Li–Si phases with increasing Li concentration: a first-principles study. *Journal of Power Sources*, 195(19):6825–6830, 2010.
- [29] Gogi K Singh, Gerbrand Ceder, and Martin Z Bazant. Intercalation dynamics in rechargeable battery materials: general theory and phase-transformation waves in lifepo 4. *Electrochimica Acta*, 53(26):7599–7613, 2008.
- [30] G Brian Stephenson. Spinodal decomposition in amorphous systems. *Journal of non-crystalline solids*, 66(3):393–427, 1984.
- [31] J-M Tarascon and Michel Armand. Issues and challenges facing rechargeable lithium batteries. *Nature*, 414(6861):359–367, 2001.
- [32] Jiang Wei Wang, Yu He, Feifei Fan, Xiao Hua Liu, Shuman Xia, Yang Liu, C. Thomas Harris, Hong Li, Jian Yu Huang, Scott X. Mao, and et al. Two-phase electrochemical lithiation in amorphous silicon. *Nano Lett.*, 13(2):709–715, Feb 2013.
- [33] M Stanley Whittingham. History, evolution, and future status of energy storage. *Proceedings of the IEEE*, 100(Special Centennial Issue):1518–1534, 2012.
- [34] Steven Wise, Junseok Kim, and John Lowengrub. Solving the regularized, strongly anisotropic Cahn-Hilliard equation by an adaptive nonlinear multigrid method. *Journal of Computational Physics*, 226(1):414 – 446, 2007.
- [35] Kejie Zhao, Georgios A. Tritsarlis, Matt Pharr, Wei L. Wang, Onyekwelu Okeke, Zhigang Suo, Joost J. Vlassak, and Efthimios Kaxiras. Reactive flow in silicon electrodes assisted by the insertion of lithium. *Nano Lett.*, 12(8):4397–4403, Aug 2012.